Using GOES-16 Time Series to characterize near real-time active fires in Cerrado

Mikhaela A. J. S. Pletsch[1], Thales Sehn Körting[1], Felipe Carraro Morita[2], Fabiano Morelli[1], Olga O. Bittencourt[1], Paulo S. S. Victorino[1]

[1]Instituto Nacional de Pesquisas Espaciais (INPE)
Caixa Postal 15.064 – 91.501-970 – São José dos Campos – SP – Brazil

{mikhaela.pletsch; thales.korting; fabiano.morelli}@inpe.br

{olga.bittencourt; paulo.victorino}@inpe.br

[2]Rocket Science Consulting
São Paulo – SP – Brazil

felipe.morita@rocketscience.com.br

Abstract. *Cerrado is the largest savanna in South America. As such, the incidence of fire in this biome is complex and diverse, requiring a range of Remote Sensing data and techniques to support its studies. The GOES-16 satellite presents an ultra high temporal resolution (one new image observation every 15 minutes), and provides insights about active fires through the Fire Temperature RGB (FT-RGB) composition. In this paper, we investigated the Time Series of the FT-RGB near and far from the active fire environments to analyze its potential to improve our comprehension about near real-time active fires in Cerrado.*

1. Introduction

The Brazilian savanna, Cerrado, is the second largest biome in South America, comprehending more than 2 million km^2, about 24% of the Brazilian territory [Ribeiro and Walter 2008, Ministério do Meio Ambiente 2009]. Cerrado holds the richest biodiversity among the tropical savannas [Sano et al. 2010], mainly because of the high range of edaphic-climatic factors, which results in a diversity of plant-available moisture regime, latitude, chemistry of the soil, geomorphology, topography, and frequency of fire processes [Cianciaruso et al. 2005, Ribeiro and Walter 2008]. The role of Cerrado is not limited to biodiversity, it also includes food security [Klink and Moreira 2002], being one of the top grain and beef-producing regions in the world [Pereira et al. 2012]. From this perspective, biodiversity and agriculture aspects unravel Cerrado's importance, although only 6% of its native vegetation is located in integral protection areas [Françoso et al. 2015].

The severe Land Use and Land Cover Changes (LULCC) in the last few decades have been threatened Cerrado [Fearnside 2001, Beuchle et al. 2015], and the main driver of LULCC is the agricultural expansion [Gibbs et al. 2015]. Currently, it is estimated that only about 52% of Cerrado's vegetation was not affected [FIP-CERRADO 2018]. In Cerrado, natural fires are caused by thunderstorms and lightning [Ramos-Neto and Pivello 2000], but the indiscriminate use of fire for

both, to boost fresh grass growth and to open new agricultural areas [Coutinho 1990, Klink and Machado 2005, Ministério do Meio Ambiente 2014], can influence in the natural fire incidence, and impact the environment. It is estimated that due to the climate and societal changes, global fire impacts may even increase in the future, requiring thus a better spatial-temporal comprehension of this issue in order to improve the fire management [Morgan et al. 2001, Chuvieco et al. 2019].

The use of Remote Sensing (RS) for fire monitoring has been proved to be powerful and effective [Joyce et al. 2009]. It enables the acquisition of important information including location, timing, burning extent and the constant monitoring without the necessity of fieldwork [Giglio et al. 1999]. Mapping and classifying land cover are commonly done through RS data such as Landsat and Sentinel, whose in the best case scenario present a temporal resolution of once a week. However, near real-time analysis of fire incidence in large areas is essential for a deep comprehension about the dynamics of spatio-temporal patterns in Cerrado. Even tough, currently such analysis is limited to a temporal resolution of once or twice a day. In this way, a range of techniques have been developed for geosynchronous (temporal resolution of 60 min or less) satellites [Giglio et al. 1999], such as the Fire Temperature RGB (FT-RGB) composition. Launched in November 2016, the GOES-16 satellite presents an ultra high temporal resolution (05-15 minutes), and has the potential to provide insights about active fire location and behaviour through the FT-RGB.

Since there is no complete model that describes near real-time active fires in the region, we investigated in this study the potential of GOES-16 Time Series (TS) through the FT-RGB bands as a support for near real-time active fires detection and characterization in Cerrado. Two main questions guided the analysis: 1) *How does the GOES-16 TS behave in near and far from active fire environments?*; 2) *How does the GOES-16 FT-RGB compositions behave in near and far from active fire environments?*. For that, we assessed the FT-RGB bands behaviour in a study area of about 3,000 km^2 located in Tocantins State during one day (October 24th, 2018) in the Cerrado biome.

2. Background

2.1. Active Fires: Theory and Sensors

The active fire products (*hot spots*) are able to detect and characterize current fire spots. The most indicated wavelength value for active fire detection is centered near 4 μm (middle infrared) in absolute terms and also comparatively with the band around 11 μm (thermal infrared), once the latter corrects the surface temperature from the atmospheric and emissivity influences [Robinson 1991, Pereira et al. 1997, Giglio et al. 2003, Giglio et al. 2008, Calle and Casanova 2008]. In this manner, to visually identify a fire, the temperature difference between both bands must be roughly 10°-15°C, or about 2% of the pixel area [Weaver et al. 2004]. In GOES-16 FT-RGB bands, the area of the pixel is 4 km^2 (spatial resolution of 2 km), which would require a fire of at least 0.08 km^2 to be detected by the GOES-16. As such, even though a fire occupies just a fraction of the pixel, it can increase the brightness in the entire pixel, which indicates that low spatial resolution data are also suitable for this task. However, the flux of radiance should be sufficient to be detected, but not so intense to cause saturation in the pixel [Robinson 1991, Weaver et al. 2004].

Different sensors present advantages and disadvantages for fire behaviour description [Morgan et al. 2001] (Table 1). The Moderate Resolution Imaging Spectrometer (MODIS) was the first instrument with specific band characteristics for fire detection. Aboard NASA's Earth Observing System - Terra and Aqua, MODIS is a sun-synchronous orbit sensor, with 36 bands, and spatial resolution of 250 m, 500 m, and 1 km, and temporal resolution from 1 to 2 days [Justice et al. 2002]. VIIRS (Visible Infrared Imaging Radiometer Suite) presents 22 channels, a spatial resolution of 375-750 m, and temporal resolution of 1-2 days. It was created to ensure continuity of MODIS observations [Justice et al. 2013]. VIIRS is aboard the joint NASA/NOAA satellite, the Suomi National Polar-orbiting Partnership (S-NPP). Besides, the Geostationary Operational Environmental Satellite system (GOES) is a joint effort of NASA and NOAA and comprehends a constellation of satellites. The GOES-16 was launched in November 2016, carrying the multispectral imager instrument Advanced Baseline Imager (ABI). It provides 16 bands with temporal resolution of 05-15 minutes and has a spatial resolution of 0.5 to 2 km. The global Wild Fire Automated Biomass Burning Algorithm (WF-ABBA) has been continuously improved for GOES-16 ABI characteristics, whose fire products are based also on active fire detection [Hoffman et al. 2011].

Table 1. Main current coarse spatial resolution sensors for fire analysis.

Sensor (satellite)	Resolution		
	Spectral (number of bands)	Spatial (m)	Temporal
MODIS (Aqua and Terra)	36	250-1,000	1-2 days
VIIRS (S-NPP)	22	375-750	1-2 days
ABI (GOES-16)	16	500-2,000	05-15 minutes

Figure 1 presents monthly amounts of active fires detected by Aqua, Terra, S-NPP and GOES-16 satellites in 2018 along Cerrado. Although GOES-16 data pursue an ultra high temporal resolution, its inherent characteristics does not enable the amount of detected active fire products be superior to the S-NPP, yet it is higher than the MODIS (Aqua and Terra) active fire data. From October to March, it is a rainy season and images frequently contain high clouds percentage. In these months, the use of successive images is low and the number of real burnings is small. Thus, the pattern of active fires presented in Figure 1 is also in agree with previous studies that show the concentration of active fires in the end of the dry season, mainly in September and October, since there is a precipitation deficit, small clouds percentage, and extreme vegetation conditions [Mataveli et al. 2017, Mataveli et al. 2018]. In this context, the analysis of the GOES-16 TS potential as a support for near real-time active fires detection and characterization by means of the FT-RGB bands is essential.

2.2. Fire Temperature RGB (FT-RGB)

Aiming to detect fires, GOES-16 has additional ABI bands in the near- and shortwave infrared (Table 2). While the True Color RGB is used to show the fire smokes, such bands can indicate active fire location and behaviour. Using the bands 7, 6, and 5 in a RGB composition (R7;G6;B5), hot spots and fires are highlighted in red, orange, yellow or white, as the fire get hotter and the pixels become saturated, and according to the fire size. Green and blue shades can be related to ice and water clouds, respectively [SPoRT 2018].

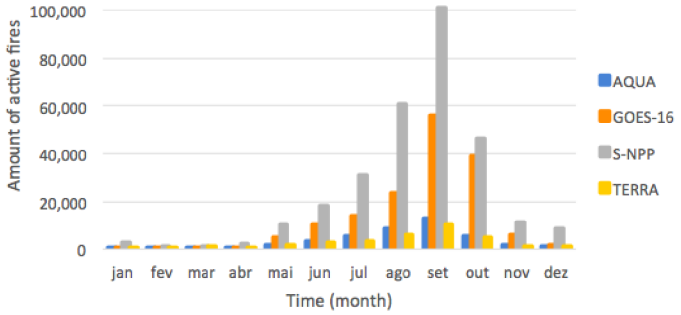

Figure 1. Amount of active fire detected by different satellites in 2018 along Cerrado.

Some limitations of the application are the presence of clouds, which can hide fire signals, the possible false *red* fires in more dry regions [SPoRT 2018], and the color variations along days, seasons and localization [Seaman et al. 2017, Schmidt 2019]. Finally, due to the possibility of a more frequent data acquisition [Lindley et al. 2016], the incorporation of TS analysis in FT-RGB bands is a novel approach by itself.

Table 2. GOES-16 spectral bands used in a FT-RGB composition. Adapted from [SPoRT 2018].

Band	Color	Band central wavelength ($\mu\ m$)	Contribution to a saturated pixel	Fire Temperature
7	R	3.9	Hot land surface	Low
6	G	2.2	Small ice/ water particles	Medium
5	B	1.6	Water clouds	High

3. Materials and Methods

3.1. Study Area

According to the climate Köppen-Geiger classification, Cerrado predominantly presents dry winter (Aw), April-September, and hot summer (Cwa), October-March [Peel et al. 2007, Ribeiro and Walter 2008, Alvares et al. 2013]. This environment presents average annual precipitation ranging from 1,300 to 1,600 mm, and temperature of 20,1 °C [Ribeiro and Walter 2008], yet both vary over the years [Ferreira et al. 2018].

The study area comprehends about 3,000 km^2. Located on the borders of the Paranã, Conceição do Tocantins, and Arraias municipalities in Tocantins State, Brazil in Cerrado biome (Figure 2). The area was selected considering the condensed presence of active fires data from different satellites and the relative homogeneous natural land cover according to the 2013 TerraClass Cerrado classification (path/row: 221/069) [Ministério do Meio Ambiente 2015].

3.2. Dataset

Two main datasets were used in this study, GOES-16 spectral bands and active fire products. The python package GOESPY was used to download the dataset from the GOES-16

Figure 2. Localization of the Study Area among the three biggest biomes in Brazil.

satellite on the AWS (Amazon Web Services) [Mello 2018]. For the FT-RGB composition, the Level 2 spectral ABI bands 05, 06, and 07 were acquired for the whole day of October 24th, 2018. The TS was composed by 288 scenes, 96 from each band, with temporal resolution of 15 minutes. Besides, the bands 01, 02, and 03 were also acquired in order to support the analysis in a True Color RGB composition (R2;G3;B1).

The active fire products were acquired through the Program of Burns and Forest Fires Monitoring[1] (*Programa Queimadas*), which is a project coordinated by Brazilian National Institute for Space Research (INPE). In the study area, a total of 36 spots presented active fires in October 24th, 2018, however only 33 were analyzed, which were acquired between 2:00 pm and 5:59 pm (interval of interest) from the S-NPP, Aqua and Terra satellites.

3.3. Methods

After the dataset acquision, due to the spatial resolution difference between band 5 (1 km), and bands 6 and 7 (2 km), a digital image processing was performed on the band 5 aiming to resampled it to 2 km. In this way, a moving average filter with window of size 4x4 was performed and the highest value was obtained.

Later to the aforementioned image processing step, we performed a different approach to each guide question, which analyses were supported by the True Color RGB composition. For the first question (*How does the GOES-16 TS behave in near and far from active fire environments?*), we performed a TS analysis of the FT-RGB bands for a whole day, near (< 3.0 km), and far (> 6.0 km) from active fires pixels, due to the homogeneity within each group. Data between 3.0 and 6.0 km presented more heterogenous

[1]Freely available at: `www.inpe.br/queimadas`

data and were not analyzed in this study. In this manner, the average of the pixels were temporally analyzed.

For the second question (*How does the GOES-16 FT-RGB compositions behave in near and far from active fire environments?*), we analyzed the behaviour of the FT-RGB composition between 2:00 pm and 5:59 pm for the whole study area, comprehending the fire behaviour and its relation to the active fire products. Furthermore, three different analyses were conducted in detail along the period.

4. Results and Discussion

4.1. How does the GOES-16 TS behave in near and far from active fire environments?

The bands 5 (B05) and 6 (B06) do not present information from 9:00 pm to 8:00 am due to the lack of daylight, while band 7 (B07) does. Even tough, this period was not analyzed in B07, once there was no True Color composition to support the analysis (Figure 3).

The B05 TS curve presented a quite similar behaviour in near (NAF) and far from active fires (FAF) spectral curves along the day, with peaks around 10:00 am and 4:00 pm (Figure 3-A). From 8:00 am to about 12:00 pm, the area presented dense clouds, which may have affected the band curve in this period. During the time interval between 2:00 pm and 4:00 pm, the NAF values were higher (Figure 3-B), which may indicate that the presence of active fires increases the values in this band.

TS of B06 data also presents an analogous pattern to the B05, with peaks in both curves, NAF and FAF, around 10:00 am and 4:00 pm (Figure 3-C). The first one can be also due to the presence of clouds. The second peak as well as B05, NAF values are superior. At 5:00 pm, as well as in B05, there is a decrease in the values, probably due to the sunset and the inherit sensor characteristics (Figure 3-D). Both bands can be physically related to aerosol particle size, and specially the B06 primary use was hot spot detection at emission temperatures greater than 600 K.

Differently from the aforementioned bands, the B07 values pursue another pattern along the time, and it was not possible to identify an influence of the clouds around 10 am. B07 TS presented just a soft peak curve from 9:00 am to 9:00 pm (Figure 3-E), which can be explained considering this band contains daytime solar reflectance component. Along it, it seems that the curves NAF and FAF are overlapped. Nonetheless, a closer analysis between 2:00 pm and 5:59 pm shows that the curves are slightly different, and the NAF values are again higher (Figure 3-F).

Such results could support the development of a reliable process able to classify GOES-16 based on the spectral-temporal characteristics. However, the use of nearer pixels ($<$3 km) may distinguish the results of NAF and FAF even better. Furthermore, the aforementioned bands main advantage is in RGB composition, but GOES-16 presents 16 different bands. As such, it would be suitable to develop an approach, as an index that can use the full potential of the integrated bands. For instance, the use of a middle infrared band (B07) may be even boosted when integrated with the a thermal infrared band (Band 14 in the case of GOES-16), as showed in Section 2.1. Moreover, the analysis of FAF temporal patterns could benefit the identification of anomalies in TS that can be related to the incidence of fires.

Figure 3. TS spectral behaviour of the average values of the GOES-16 FT-RGB bands near and far from active fire environments - October 24th, 2018. A highlight is available during the acquisition of active fire data (2: pm - 5:00 pm). A. Band 5 (B05) along a whole day; B. B05 from 2:00 pm to 5:59 pm - interval with detected active fires; C. Band 6 (B06) along a whole day; D. B06 from 2:00 pm to 5:59 pm - interval with detected active fires; E. Band 7 (B07) along a whole day; F. B07 from 2:00 pm to 5:59 pm - interval with detected active fires.

4.2. How does the GOES-16 FT-RGB compositions behave in near and far from active fire environments?

According to the FT-RGB quick guide [SPoRT 2018], colors derived from the composition can be related to different targets. In theory, near black color is more related to water/snow/night, shapes of blue to water clouds, green to ice clouds, purples/pinks to

clear land, red to *warm* fire, and shades of maroon to burn scars. However, for the same target the presented color may vary in space and time.

Along the day, the True Color RGB composition enabled the identification of just three different targets Cerrado natural vegetation, cloud, and clouds shadow. In general, the presence of clouds were highly accurate with the pixels in shades of blue and green, which hide sometimes the land cover. The FT-RGB could identify a small water course in the north of the scene mainly from 2:00 pm to 2:45 pm (Figure 4). As the size of the water course is too small, possibly there are contributions from others factors for the amount of near black pixels.

Due to the complexity of the TS, we are going to present in detail three different analysis. In the first one (Figure 4, white dotted square), it is possible to notice at 2:00 pm the presence of a red pixel in the center of the square, which is classified as a source of active fire by the satellites Terra at 2:15 pm, and S-NPP at 3:48 pm. Except for the presence of cloud or cloud shadow, this pixel remained with a hot color palette during the whole analyzed interval.

The second analysis (Figure 4, dark blue dotted square) also presented in the center of the square a pixel with shades of red, orange, pink, and purple. It was identified active fire in this pixel or in the adjacent pixel above at 5:00 pm and 5:30 pm, by the satellites Aqua and S-NPP, respectively. As it is located in in the extreme southwest of the area, region that present some clouds along the afternoon, the result may be influenced by this target. The last analysis (Figure 4, orange dotted square) is regarding two adjacent pixels in the center of the square, whose color along the period was also red, orange, pink, and purple. It was identified active fire by the satellites S-NPP at 3:48 pm, Aqua at 5:00 pm, and in the adjacent pixel above by the S-NPP at 5:30 pm.

Due to the spatio-temporal variations of the colors in the FT-RGB composition, it would be necessary to assess the correlation between the targets and the possible correspondent band values in Cerrado. Furthermore, the presence of water clouds could have influenced the analysis of the red pixels and the active fire spots. Such process would be crucial to identify which values of the RGB could endorse the presence of fire.

5. Conclusion

In this study, we analyzed the use of GOES-16 TS to characterize near real-time active fires in Cerrado. As a result, we identified a certain pattern along the 24 hours TS from bands 05, 06, and 07. However, the TS curve analysis was influenced by the presence of clouds from 8:00 am to 12:00 pm. During the presence of active fires (2:00 pm - 5:59 pm), the NAF values tend to be slightly higher than FAF, which may indicate that techniques of digital image processing could strength the differences and separate both groups to improve the active fire detection.

Regarding the FT-RGB composition, we visually identified a certain relation of: i) shades of red with active fires; ii) shades of blue and green with clouds; iii) the color black with the presence of water; iv) shades of brown with clear sky. For a deeper analysis of active fires, the presence of water clouds were a hindrance to better relate the color with the target. Moreover, we identified as a limitation of the technique the minimum and maximum RGB values, which presents a spatio-temporal variation, and may influence the final color.

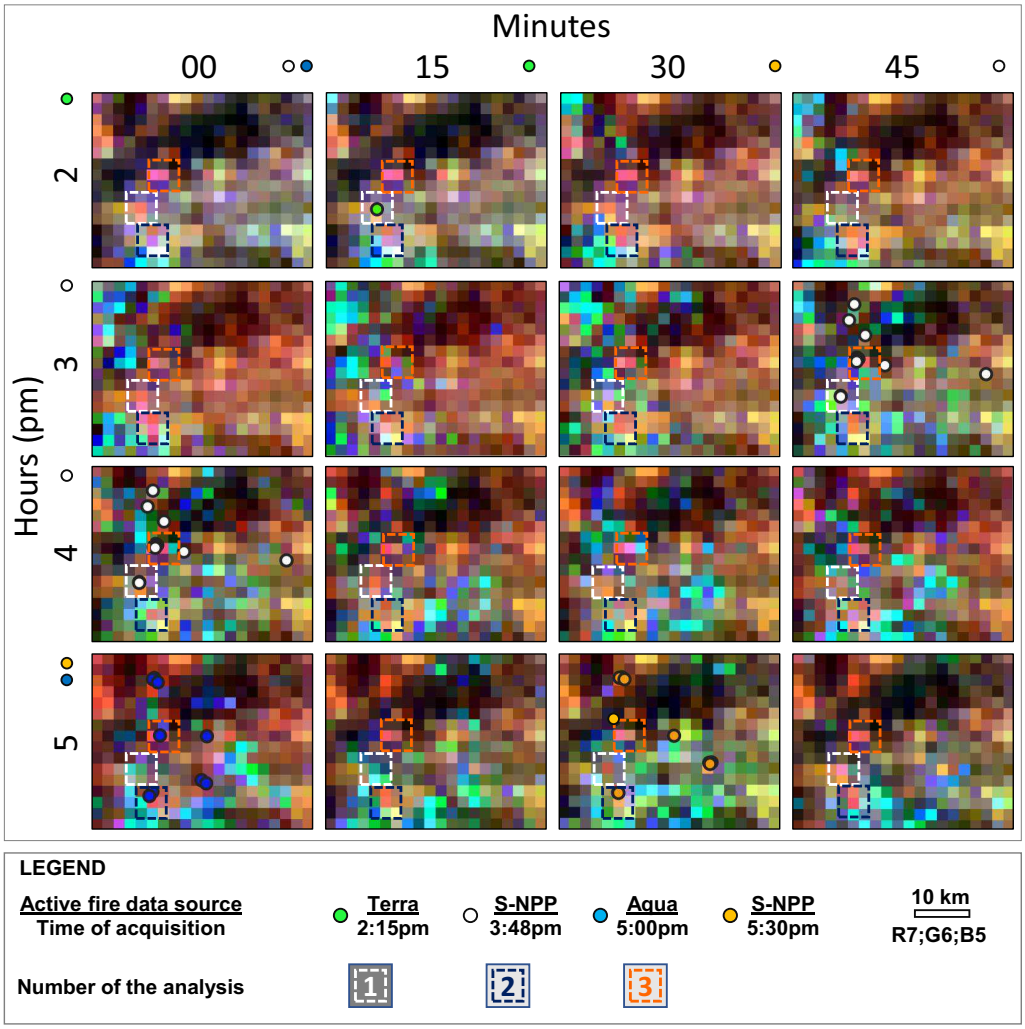

Figure 4. GOES-16 FT-RGB compositions near and far from active fire environments along October 24th, 2018, from 2:00 pm to 5:45 pm.

As part of a study already in progress, we are working on the comprehension of the spectral-temporal behaviour of the GOES-16 to assess its viability to detect near real-time active fires. The aforementioned preliminary results indicate that it is possible to develop an approach to use this sensor data to detect or improve the active fires indication. Nonetheless, further studies are required to acknowledge such assumption. As such, we suggest: i) to analyse the remaining GOES-16 bands in larger areas focusing on the development of algorithms, such as indexes; ii) to find alternatives and to better comprehend the influence of clouds in the analyzed targets, and; iii) to incorporate other related data products as active fire data from the Advanced Very High Resolution Radiometer (AVHRR), to generate models that can more accurately distinguish active fires.

Acknowledgments

The authors would like to thank the financial support to the National Council for Scientific and Technological Development (CNPq), process 140377/2018-2, the Coordination for the Improvement of Higher Education Personnel (CAPES), code 001, the Coordination of Associated Laboratories - CLA/INPE, process 300587/2017-1, and the São Paulo Research Foundation (FAPESP), grant #2017/24086-2.

References

Alvares, C. A., Stape, J. L., Sentelhas, P. C., de Moraes, G., Leonardo, J., and Sparovek, G. (2013). Köppen's climate classification map for brazil. *Meteorologische Zeitschrift*, 22(6):711–728.

Beuchle, R., Grecchi, R. C., Shimabukuro, Y. E., Seliger, R., Eva, H. D., Sano, E., and Achard, F. (2015). Land cover changes in the Brazilian Cerrado and Caatinga biomes from 1990 to 2010 based on a systematic remote sensing sampling approach. *Applied Geography*, 58:116–127.

Calle, A. and Casanova, J.-L. (2008). Forest fires and remote sensing. In *Integration of Information for Environmental Security*, pages 247–290. Springer.

Chuvieco, E., Mouillot, F., van der Werf, G. R., San Miguel, J., Tanasse, M., Koutsias, N., García, M., Yebra, M., Padilla, M., Gitas, I., et al. (2019). Historical background and current developments for mapping burned area from satellite earth observation. *Remote Sensing of Environment*, 225:45–64.

Cianciaruso, M. V., Batalha, M. A., and da Silva, I. A. (2005). Seasonal variation of a hyperseasonal cerrado in emas national park, central brazil. *Flora-Morphology, Distribution, Functional Ecology of Plants*, 200(4):345–353.

Coutinho, L. M. (1990). Fire in the ecology of the brazilian cerrado. In *Fire in the tropical biota*, pages 82–105. Springer.

Fearnside, P. M. (2001). Soybean cultivation as a threat to the environment in brazil. *Environmental Conservation*, 28(1):23–38.

Ferreira, D. H. L., Badinger, A., and Tendolini, J. C. (2018). Distribuições de tendências sazonais de temperatura média e precipitação nos biomas brasileiros. *Revista Brasileira de Meteorologia*, 33(1):97–113.

FIP-CERRADO, F. I. P. (2018). Projeto de desenvolvimento de sistemas de prevenção de incêndios florestais e monitoramento da cobertura vegetal no cerrado brasileiro.

Françoso, R. D., Brandão, R., Nogueira, C. C., Salmona, Y. B., Machado, R. B., and Colli, G. R. (2015). Habitat loss and the effectiveness of protected areas in the Cerrado Biodiversity Hotspot. *Natureza e Conservacao*, 13(1):35–40.

Gibbs, H. K., Rausch, L., Munger, J., Schelly, I., Morton, D. C., Noojipady, P., Soares-Filho, B., Barreto, P., Micol, L., and Walker, N. F. (2015). Brazil's soy moratorium. *Science*, 347(6220):377–378.

Giglio, L., Csiszar, I., Restás, Á., Morisette, J. T., Schroeder, W., Morton, D., and Justice, C. O. (2008). Active fire detection and characterization with the advanced spaceborne

thermal emission and reflection radiometer (aster). *Remote Sensing of Environment*, 112(6):3055–3063.

Giglio, L., Descloitres, J., Justice, C. O., and Kaufman, Y. J. (2003). An enhanced contextual fire detection algorithm for modis. *Remote sensing of environment*, 87(2-3):273–282.

Giglio, L., Kendall, J., and Justice, C. (1999). Evaluation of global fire detection algorithms using simulated avhrr infrared data. *International Journal of Remote Sensing*, 20(10):1947–1985.

Hoffman, J., Schmidt, C., Prins, E., and Brunner, J. (2011). The GOES-R ABI Wild Fire Automated Biomass Burning Algorithm. *AGU Fall Meeting Abstracts*, pages 1636–.

Joyce, K. E., Belliss, S. E., Samsonov, S. V., McNeill, S. J., and Glassey, P. J. (2009). A review of the status of satellite remote sensing and image processing techniques for mapping natural hazards and disasters. *Progress in Physical Geography*, 33(2):183–207.

Justice, C., Giglio, L., Korontzi, S., Owens, J., Morisette, J., Roy, D., Descloitres, J., Alleaume, S., Petitcolin, F., and Kaufman, Y. (2002). The modis fire products. *Remote Sensing of Environment*, 83(1-2):244–262.

Justice, C. O., Román, M. O., Csiszar, I., Vermote, E. F., Wolfe, R. E., Hook, S. J., Friedl, M., Wang, Z., Schaaf, C. B., Miura, T., et al. (2013). Land and cryosphere products from Suomi NPP VIIRS: Overview and status. *Journal of Geophysical Research: Atmospheres*, 118(17):9753–9765.

Klink, C. A. and Machado, R. B. (2005). A conservação do cerrado brasileiro. *Megadiversidade*, 1(1):147–155.

Klink, C. A. and Moreira, A. G. (2002). Past and current human occupation, and land use. *The cerrados of Brazil: ecology and natural history of a neotropical savanna*, pages 69–88.

Lindley, T., Anderson, A. R., Mahale, V. N., Curl, T. S., Line, W. E., Lindstrom, S. S., and Bachmeier, A. S. (2016). Wildfire detection notifications for impact-based decision support services in oklahoma using geostationary super rapid scan satellite imagery. *Journal of Operational Meteorology*, 4(14).

Mataveli, G. A. V., Silva, M. E. S., Pereira, G., da Silva, F., Cardozo, F. S. K., Bertani, G., Costa, J. C., de Cássia Ramos, R., and da Silva, V. V. (2017). Analysis of fire dynamics in the brazilian savannas. *Natural Hazards and Earth System Sciences Discussions*, pages 1–27.

Mataveli, G. A. V., Silva, M. E. S., Pereira, G., da Silva Cardozo, F., Kawakubo, F. S., Bertani, G., Costa, J. C., de Cássia Ramos, R., and da Silva, V. V. (2018). Satellite observations for describing fire patterns and climate-related fire drivers in the brazilian savannas. *Natural Hazards and Earth System Sciences*, 18(1):125.

Mello, P. A. d. S. (2018). goes-py. Available in: pypi.org/project/goespy, accessed in 8 oct. 2019.

Ministério do Meio Ambiente (2009). *Plano de ação para prevenção e controle do desmatamento e das queimadas no cerrado - PPCerrado*. MMA.

Ministério do Meio Ambiente (2014). *PPCerrado – Plano de ação para prevenção e controle do desmatamento e das queimadas no Cerrado: 2 fase (2014-2015)*. MMA.

Ministério do Meio Ambiente (2015). *Mapeamento do Uso e Cobertura da Terra do Cerrado - Projeto TerraClass Cerrado 2013*. Brasil, Brasília.

Morgan, P., Hardy, C. C., Swetnam, T. W., Rollins, M. G., and Long, D. G. (2001). Mapping fire regimes across time and space: understanding coarse and fine-scale fire patterns. *International Journal of Wildland Fire*, 10(4):329–342.

Peel, M. C., Finlayson, B. L., and McMahon, T. A. (2007). Updated world map of the köppen-geiger climate classification. *Hydrology and earth system sciences discussions*, 4(2):439–473.

Pereira, J., Chuvieco, E., Beaudoin, A., and Desbois, N. (1997). Remote sensing of burned areas: A review. a review of remote sensing methods for the study of large wildland fires. *Report of the Mega fires Project ENV-CT. Departamento de Geografía, Universidad de Alcalá*, pages 127–184.

Pereira, P. A. A., Martha, G. B., Santana, C. A., and Alves, E. (2012). The development of brazilian agriculture: future technological challenges and opportunities. *Agriculture & Food Security*, 1(1):4.

Ramos-Neto, M. B. and Pivello, V. R. (2000). Lightning fires in a brazilian savanna national park: rethinking management strategies. *Environmental management*, 26(6):675–684.

Ribeiro, J. F. and Walter, B. M. T. (2008). As principais fitofisionomias do bioma cerrado. *Cerrado: ecologia e flora*, 1:151–212.

Robinson, J. M. (1991). Fire from space: Global fire evaluation using infrared remote sensing. *International Journal of Remote Sensing*, 12(1):3–24.

Sano, E. E., Rosa, R., Brito, J. L. S., and Ferreira, L. G. (2010). Land cover mapping of the tropical savanna region in Brazil. *Environmental Monitoring and Assessment*, 166(1-4):113–124.

Schmidt, C. (2019). GOES-R Fire Detection and Characterization Fact Sheet. Technical report, NOAA, National Oceanic & Atmospheric Administration.

Seaman, C. J., Miller, S. D., Lindsey, D. T., and Hillger, D. W. (2017). Jpss and goes-r multispectral imagery applications and product development at cira. In McWilliams, G., Jamilkowski, M. L., Kalluri, S., Schmit, T. J., and Mango, S. A., editors, *Proceedings of 13th Annual Symposium on New Generation Operational Environmental Satellite Systems*, page 259. American Meteorological Society.

SPoRT, N. (2018). Fire Temperature RGB: Quick Guide. Technical report, NASA, National Aeronautics and Space Administration; SPoRT, Short-term Prediction Research and Transition Center.

Weaver, J. F., Lindsey, D., Bikos, D., Schmidt, C. C., and Prins, E. (2004). Fire detection using goes rapid scan imagery. *Weather and Forecasting*, 19(3):496–510.